Acta Cryst. (1996). A52, 669–674

Observation of Phase Change of X-ray Polarizability in Rocking Curves

T. FUKAMACHI,[a] R. NEGISHI,[a]* S. ZHOU,[a] M. YOSHIZAWA,[a] T. SAKAMAKI,[b] T. KAWAMURA[c] AND T. NAKAJIMA[d]

[a]*Saitama Institute of Technology, Okabe, Saitama 369-02, Japan,* [b]*JEOL Ltd, 1–2 Musashino 3-chome, Akishima, Tokyo 196, Japan,* [c]*Department of Physics, Yamanashi University, Kofu, Yamanashi 400, Japan, and* [d]*Photon Factory, KEK, Oho, Tsukuba, Ibaraki 305, Japan. E-mail: negishi@sit.ac.jp*

(*Received 7 July 1995; accepted 25 March 1996*)

Abstract

By tuning the X-ray energy from synchrotron radiation very close to the *K*-absorption edges of Ga and As, rocking curves were measured of the GaAs 200 diffraction and the transmitted beams in the symmetric Laue case. The rocking curve of the transmitted beam is asymmetric with respect to the angle of the exact Bragg condition. The asymmetry reverses as the sign of the Fourier transform of either the real or the imaginary part of the X-ray polarizability changes. From the turning point of asymmetry, the accuracy of the existing calculated values of anomalous scattering factors was examined.

1. Introduction

As an optoelectronic device, GaAs crystals have acquired much interest in the last two decades. During this period, the perfection of the crystal has been improved, making it possible to study X-ray dynamical diffraction from a GaAs crystal. Since the *K*-absorption edges of both Ga and As are in an appropriate energy range to be studied by using X-rays from synchrotron radiation, a GaAs crystal is suitable for studying X-ray resonant scattering. As an example, the X-ray resonant scattering *Pendellösung* beat has been measured for the GaAs 600 reflection (Yoshizawa, Fukamachi, Ehara, Kawamura & Hatakawa, 1988).

Fukamachi & Kawamura (1993) (hereafter FK) modified an X-ray dynamical theory of diffraction to include the case in which the Fourier of the real part of the X-ray polarizability (χ_{hr}) is zero and pointed out that the rocking curve in the Bragg case due to that of the imaginary part of the polarizability (χ_{hi}) when χ_{hr} is zero is much sharper than that due to χ_{hr} when χ_{hi} is zero. A similar effect has been studied theoretically by Kato (1992). FK also pointed out that in the Laue case the anomalous absorption effect is independent of the crystal thickness in some cases and the period of *Pendellösung* fringes is inversely proportional to $|\chi_{hi}|$.

Based on the theory by FK, Fukamachi, Negishi & Kawamura (1994, 1995) [hereafter FNK(*a*) and FNK(*b*), respectively] reported several characteristic phenomena of the resonant scattering. FNK(*a*) studied the dynamical diffraction in the Laue case and pointed out a non-transparent effect that the transmitted intensity becomes zero. They also pointed out that the anomalous transmission becomes conspicuous in the asymmetric reflection condition when χ_{hr} is zero. FNK(*b*) studied the dispersion surfaces and pointed out that the dispersion surface for $\chi_{hr} = 0$ is quite different from that for $\chi_{hi} = 0$.

In this paper, we study the relation between the change of the phase factors of χ_{hi} and χ_{hr} and the asymmetry of the rocking curves in the Laue case. First, by using calculated values, we search for an X-ray energy at which χ_{hr} is equal to $-\chi_{hi}$ in the high-energy side of the Ga *K*-absorption edge and also an energy at which $-\chi_{hr}$ is equal to $-\chi_{hi}$ just below the As *K*-absorption edge. Then we measure the rocking curves of both the transmitted and the diffracted beams at these energy points. We compare the calculated rocking curves with the measured ones and discuss a phase determination from measured rocking curves of the transmitted beam.

2. Calculations

2.1. *X-ray polarizability*

The real and the imaginary parts of X-ray polarizability χ_h are given by

$$\chi_h = \chi_{hr} + i\chi_{hi} = |\chi_{hr}| \exp(i\alpha_{hr}) + i|\chi_{hi}| \exp(i\alpha_{hi}), \quad (1)$$

where

$$\chi_{hr} = -(4\pi/v\omega^2)F_{hr},$$

and

$$\chi_{hi} = -(4\pi/v\omega^2)F_{hi}. \quad (2)$$

We use the atomic units ($\hbar = m = e = 1$). In (2), v is the unit-cell volume and ω the X-ray energy. F_{hr} and F_{hi} are the real and the imaginary parts of the crystal structure factor, respectively, which are expressed by

$$F_{hr} = \sum (f^0 + f')_j \exp(2\pi \mathbf{h} \cdot \mathbf{r}_j) T_j,$$

and

$$F_{hi} = \sum f_j'' \exp(2\pi \mathbf{h} \cdot \mathbf{r}_j) T_j. \quad (3)$$

ISSN 0108-7673

Here, f^0 is the normal atomic scattering factor, f' and f'' are the real and the imaginary parts of the anomalous scattering factor, respectively. **h** is the reciprocal-lattice vector, $\mathbf{r}_j$ the jth atom position vector and T_j the correction factor due to thermal vibration. The summation in (3) is over all atoms in a unit cell. The phase factor is defined as

$$\delta = \alpha_{hi} - \alpha_{hr}. \tag{4}$$

2.2. *Rocking curves in the symmetric Laue case*

The diffracted (P_h) and the transmitted (P_d) intensities in the symmetric Laue case are given in the two-wave approximations of the X-ray dynamical theory of diffraction as [FK, FNK(a)]

$$\begin{aligned} P_h/P_0 = \exp(-\mu H/\cos\theta_B)(1 - 2p\sin\delta) \\ \times [\sin^2(sH\,\mathrm{Re}\,L^{1/2}) \\ + \sinh^2(sH\,\mathrm{Im}\,L^{1/2})]/|L^{1/2}|^2 \end{aligned} \tag{5}$$

and

$$\begin{aligned} P_d/P_0 = \exp(-\mu H/\cos\theta_B)\{[(|L^{1/2}|^2 - W^2) \\ \times \cos(2sH\,\mathrm{Re}\,L^{1/2}) \\ + (|L^{1/2}|^2 + W^2)\cosh(2sH\,\mathrm{Im}\,L^{1/2})]/2 \\ + W\,\mathrm{Im}\,L^{1/2}\sin(2sH\,\mathrm{Re}\,L^{1/2}) \\ - W\,\mathrm{Re}\,L^{1/2}\sinh(2sH\,\mathrm{Im}\,L^{1/2})\}/|L^{1/2}|^2. \end{aligned} \tag{6}$$

Here, μ is the linear absorption coefficient, θ_B the Bragg angle and H the crystal thickness. The parameters s and W are given by

$$s = \pi\kappa_{or}(|\chi_{hr}|^2 + |\chi_{hi}|^2)^{1/2}/\cos\theta_B \tag{7}$$

$$W = (\theta_B - \theta)\sin 2\theta_B/(|\chi_{hr}|^2 + |\chi_{hi}|^2)^{1/2}, \tag{8}$$

with κ_{or} the incident wave number in a crystal and θ the incident angle. If we use

$$A = W^2 + 1 - b^2 \tag{9}$$

and

$$B = 2p\cos\delta, \tag{10}$$

the quantity $|L^{1/2}|$ is expressed as

$$|L^{1/2}|^2 = (A^2 + B^2)^{1/2}. \tag{11}$$

The real and the imaginary parts of $L^{1/2}$ are then given by

$$\mathrm{Re}\,L^{1/2} = (A + |L^{1/2}|^2)^{1/2}/2^{1/2} \tag{12}$$

and

$$\mathrm{Im}\,L^{1/2} = \pm(-A + |L^{1/2}|^2)^{1/2}/2^{1/2}. \tag{13}$$

It is convenient to use a parameter q defined as

$$q = 1/[1 + (|\chi_{hr}|/|\chi_{hi}|)^2]. \tag{14}$$

Then the quantities b and p in (9) and (10) are

$$b = (2q)^{1/2}, \tag{15}$$

$$p = [q(1-q)]^{1/2}. \tag{16}$$

For the double sign in (13), the positive is taken when $p\cos\delta > 0$ and the negative is taken when $p\cos\delta < 0$.

For a reflection for which the relation $F_h = F_{-h}$ holds, α_{hr} and α_{hi} are either 0 or π, then δ is either 0 or $\pm\pi$. The rocking curve of the diffracted beam does not change with the change of δ because $\sin\delta$ is zero. The transmitted beam, on the other hand, changes with the change of δ, as $\cos\delta$ in (10) is either 1 or -1 and the sign in (13) changes accordingly. This does not happen when $q = 0$ ($\chi_{hi} = 0$) and $q = 1$ ($\chi_{hr} = 0$).

In Fig. 1, the rocking curves are shown for the transmitted beam and the diffracted beam when $q = 0.5$, $g_0 = \chi_{0i}/|\chi_{hi}| = -1.0$ and $sH = \pi/2$. The rocking curve (dashed line) of the transmitted beam for $\delta = 0$ is asymmetric with respect to $W = 0$: the intensity is higher for $W < 0$ than for $W > 0$. The rocking curve (solid line) of the transmitted beam for $\delta = \pi$ is obtainable by reversing the rocking curve with respect to $W = 0$. The diffracted intensity (thin solid line) is the same for $\delta =$

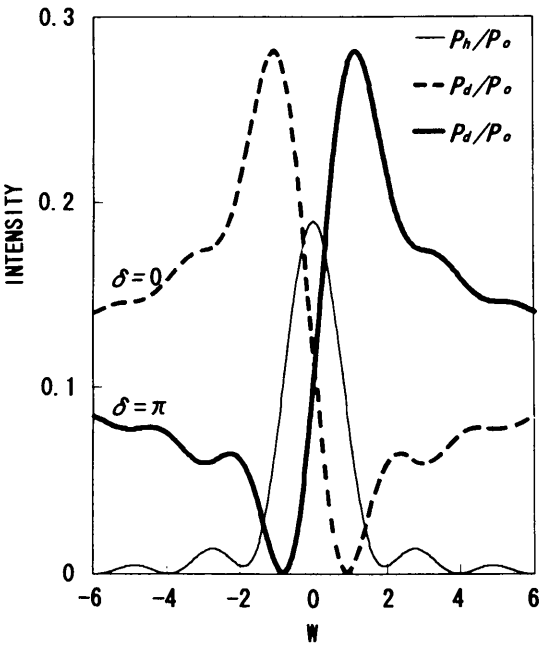

Fig. 1. The calculated rocking curves in the symmetric Laue case for $q = 0.5$, $g_0 = -1.0$ and $sH = \pi/2$. The thin solid line is the curve of the diffracted beam. The thick solid and dashed lines are the curves of the transmitted beam for $\delta = \pi$ and 0, respectively.

0 and π. The rocking curve of the diffracted beam is of symmetric form with respect to $W = 0$. All the peaks of the rocking curves are due to anomalous transmission.

In Fig. 2, similar rocking curves for $q = 0.05$, $g_0 = -1.0$ and $sH = \pi/2$ are shown. The asymmetry of the rocking curves of the transmitted beam and the symmetry of that of the diffracted beams are the same as in Fig. 1. At $W = 0$, the diffracted intensity becomes high while the transmitted intensity becomes low. *Pendellösung* fringes are clearly seen in both the transmitted and the diffracted beams in Figs. 1 and 2.

The ratio between the intensities at $W = 6$ and at $W = -6$ for $\delta = 0$ is *ca* 1.7 when $q = 0.5$, while that for $q = 0.05$ is 1.2. FNK(*a*) have pointed out that the asymmetry is largest when $q = 0.5$. Figs. 1 and 2 clearly show that the value of the phase factor δ can be determined by measuring the rocking curves of the transmitted beam in the Laue case.

When we denote the electric field of the incident X-ray as $\mathbf{E}_0$ and the electric displacement of the jth branch of the transmitted beam in a crystal as $\mathbf{D}_0^{(j)}$, we have the relation

$$\mathbf{D}_0^{(j)} = (\mathbf{E}_0/2)[1 + (-1)^{j-1} W/(1 + W^2)^{1/2}] \quad (17)$$

in the case of $q \gg 1$. In this case, if we average the oscillatory terms including sH in (6), we obtain the transmitted intensity (P_d) in terms of that for each branch, *i.e.*

$$P_d = P_d^{(1)} + P_d^{(2)}. \quad (18)$$

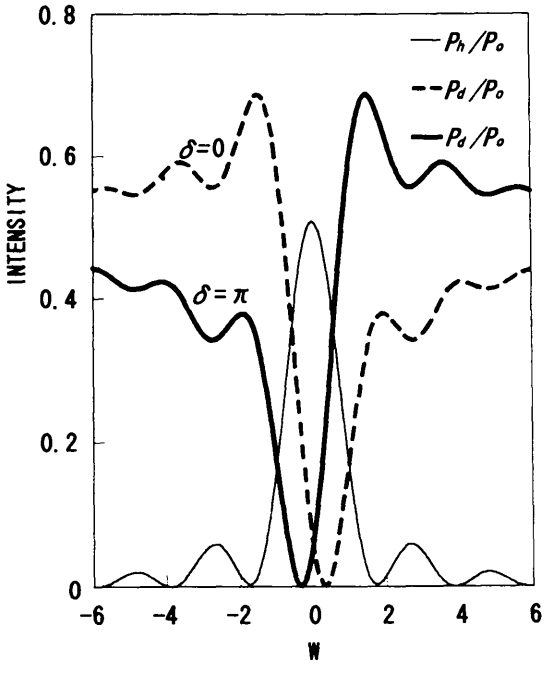

Fig. 2. The calculated rocking curves in the symmetric Laue case for $q = 0.05$, $g_0 = -1.0$ and $sH = \pi/2$. The curves are labelled the same as in Fig. 1.

Here,

$$P_d^{(j)} = |\mathbf{D}_0^{(j)}|^2 \exp\Big((-\mu H/\cos\theta_B)\{1 + (-1)^{j-1} \times \cos\delta/[|g_0|(1 + W^2)^{1/2}]\}\Big). \quad (19)$$

The meaning of (19) can be considered by looking at the complex dispersion surface [FNK(*b*)] shown in Fig. 3. The thick solid lines represent the real part (Y') of Y and the dashed lines represent the imaginary part (Z'). The real parts (Y') for branches 1 and 2 are independent of $\cos\delta$. The imaginary parts (Z') depend on $\cos\delta$. When $\delta = 0$, the value of $|Z'|$ is smaller for the branch $j = 2$ than for $j = 1$. When $\delta = \pi$, on the other hand, the value of $|Z'|$ is smaller for the branch $j = 1$. For the branch of smaller value of $|Z'|$, the anomalous transmission is observed, and for the branch of larger $|Z'|$, the anomalous absorption is observed. The term in $D_0^{(2)}$ mainly contributes the intensity in the range $W < 1$ when $\delta = 0$, and the term in $D_0^{(1)}$ contributes in the range $W > 1$ when $\delta = \pi$. The change in the form of the rocking curves for $\delta = 0$ and π occurs accordingly. The diffracted intensity is proportional to the cross term $D_0^{(1)} D_0^{(2)}$ and depends on both branches equally. The intensity does not depend on the term $\cos\delta$.

2.3. χ_{hr} *and* χ_{hi} *for GaAs 200*

In Fig. 4, the calculated values of χ_{hr} and χ_{hi} for GaAs 200 when a Ga atom sits at the origin are shown in the energy range in which the K-absorption edges of both Ga and As are contained. In the calculation, we

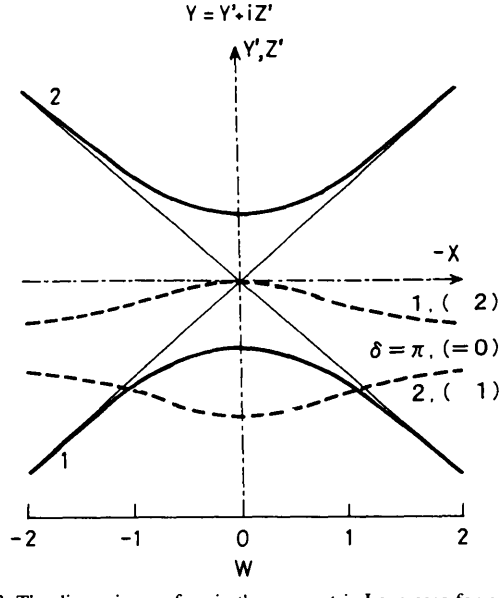

Fig. 3. The dispersion surface in the symmetric Laue case for $q = 0.5$, $g_0 = -1.0$. The ordinates Y' and Z' are the real and imaginary parts. The solid curves are the dispersion surface in the $Y'X$ plane and the dashed curves that in the $Z'X$ plane.

used the relation of Parratt & Hempstead (1954) with the oscillator strength given by Cromer (1965), which is abbreviated as PH hereafter. The dotted line shows the values of χ_h (= χ_{hr}) without the resonant scattering factors and is always positive. The thick solid curve (*a*) and the thin solid curve (*b*) are χ_{hr} and χ_{hi}, respectively, with the resonant scattering factors taken into account. Below the *K*-absorption edge of Ga [in region (1)], χ_{hr} and χ_{hi} are both positive and $\delta = 0$. Just above the Ga *K*-absorption edge [in region (2)], χ_{hi} becomes negative and $\delta = \pi$. As the energy increases further [in region (3)], χ_{hr} and χ_{hi} both become negative and $\delta = 0$. Above the As *K*-absorption edge [in region (4)], χ_{hi} becomes positive while χ_{hr} stays negative and $\delta = -\pi$.

3. Experimental results and discussion

3.1. *Measuring system and sample*

We used X-rays from synchrotron radiation at BL6C, KEK-PF, Japan. The schematic diagram of the measuring system is shown in Fig. 5. The X-rays, after passing the first slit, are monochromated by using an Si(111) double-crystal monochromator (Matsushita, Ishikawa & Oyanagi, 1986). They pass through an ion chamber as a monitor and the second slit, and are diffracted from a sample crystal. The transmitted and the diffracted X-rays are measured simultaneously by using a SSD and a scintillation counter (SC), respectively. The GaAs sample used includes 0.04 In atoms per unit cell and the EPD value is less than 500 cm^{-2}. It is a parallel plate with a thickness of 133.8 (19) μm. The X-ray energy calibration was performed by measuring an absorption spectrum of Cu foil and measuring the angle of the monochromator at the Cu *K*-absorption edge (8.980 keV).

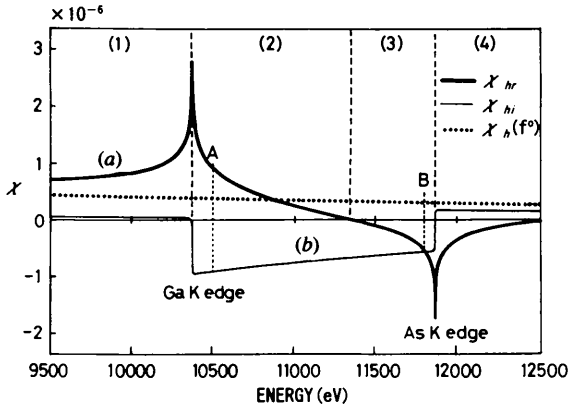

Fig. 4. χ_{hr} and χ_{hi} for GaAs 200 near the Ga and As *K*-absorption edges. The dotted line is χ_h without anomalous scattering factor.

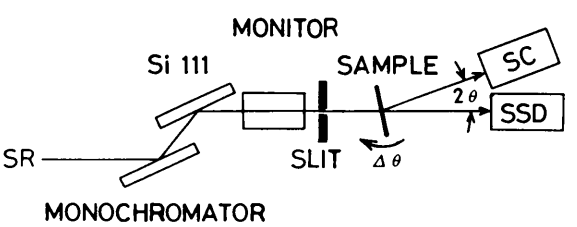

Fig. 5. Schematic diagram of the measuring system.

3.2. *Measured rocking curves*

The measured rocking curves are shown in Fig. 6. Curves in (*a*) are those measured at the energy (ω = 10.502 keV) above the Ga *K*-absorption edge at which the relation $\chi_{hr} = -\chi_{hi}$ is expected to hold (point *A* in Fig. 4). Curves in (*b*) are measured at the energy (ω = 11.805 keV) below the As *K*-absorption edge at which the relation $-\chi_{hr} = -\chi_{hi}$ is expected to hold (point *B* in Fig. 4). The thick solid curves represent the transmitted intensity and the thin solid curves the diffracted intensity. In (*a*) and (*b*), the peaks due to anomalous transmission are observed around the Bragg condition ($\Delta\theta = \theta_B - \theta = 0$) in both the transmitted and the diffracted beams. The widths of these rocking curves are *ca* 6″, which is six times larger than expected for an ideal plane wave.

It is noted that the following characteristic features are clearly observed in the rocking curves of the transmitted beam. The transmitted beam in Fig. 6(*a*) shows lower intensity in the low-angle side of the peak. The intensity increase in the low-angle side is steeper than the intensity decrease in the high-angle side. The central peak slightly shifts to the high-angle side with respect to the peak of the diffracted beam. In contrast, the intensity of the transmitted beam in (*b*) shows the reversed feature from that in (*a*). From this, we can conclude $\delta = \pi$ in (*a*) and $\delta = 0$ in (*b*), being in agreement with the theoretical expectation.

3.3. *Search for the point with* $\chi_{hi} = 0$

The sign of χ_{hi} changes from positive to negative as the X-ray energy increases from just below the Ga *K*-absorption edge to above it, as shown in Fig. 4. By comparing the measured turning point with the calculated one, we can examine the accuracy of calculated anomalous scattering factors. When χ_{hi} is zero, *i.e.* q = 0, the diffraction occurs due only to χ_{hr}. The phase of only χ_{hr} can be obtained.

In Fig. 7, the calculated χ_{hr} and χ_{hi} for GaAs 200 are shown near the Ga *K*-absorption edge. The solid curves are calculated by using f' and f'' of PH and the dashed curves are calculated by using those of Sasaki (1989) based on the method of Cromer & Liberman (1970), hereafter denoted as CLS. The turning point of χ_{hi} by the PH method is 3.7 eV below the Ga *K*-absorption edge, while that by the CLS method is just at the Ga *K* edge. Since these energies are just below the Ga *K* edge and χ_{hi} is small, the rocking curves at these energies are expected to be similar to those shown in Fig. 2.

Fig. 8 shows the measured rocking curves of the transmitted beam at -5 ± 1 eV [curve (*a*)] and -9 ± 1 eV [curve (*b*)]. The intensities in the high-angle side are higher than those in the low-angle side for curve (*a*). The relative intensities between the high- and the low-angle side are reversed for curve (*b*). We can deduce that χ_{hi} becomes zero at -7 ± 2 eV. This energy is much smaller than the values obtained by either the PH method or the CLS method. By considering the results in Fig. 2, we find that δ is π for curve (*a*) and zero for curve (*b*).

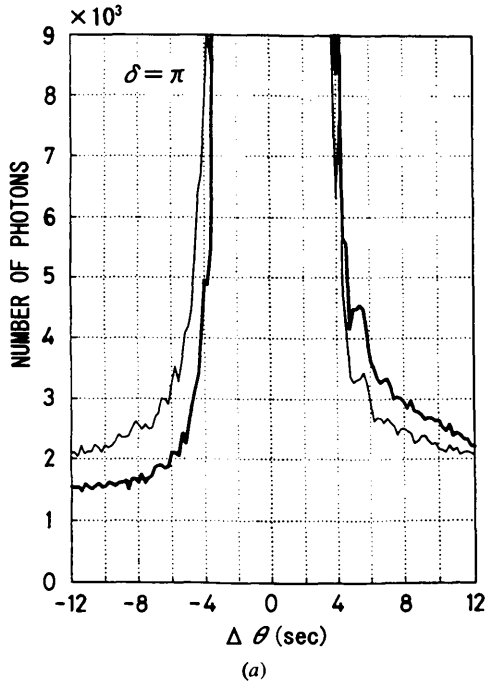

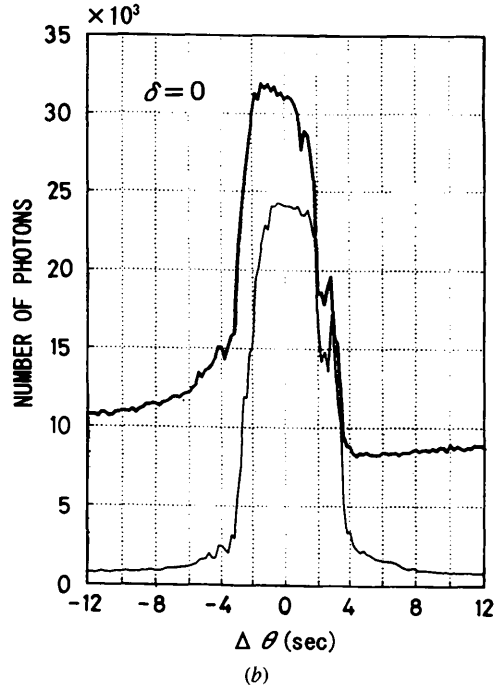

Fig. 6. The measured rocking curves for GaAs 200 at (*a*) point *A* and (*b*) point *B* in Fig. 4. The thick lines are the curve of the transmitted beam and the thin lines that of the diffracted beam.

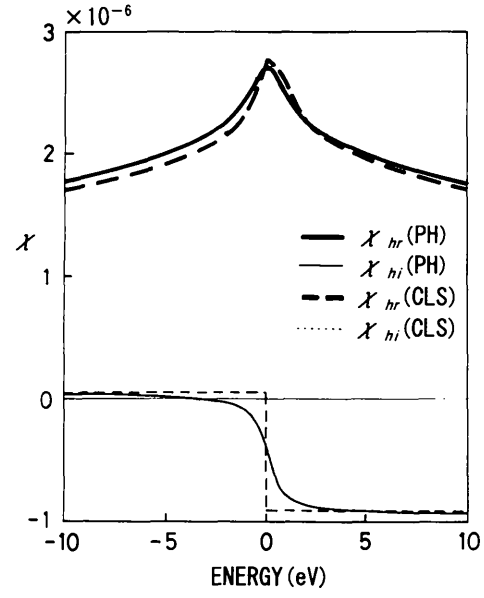

Fig. 7. The calculated values of χ_{hr} and χ_{hi} for GaAs 200 very near the Ga *K*-absorption edge.

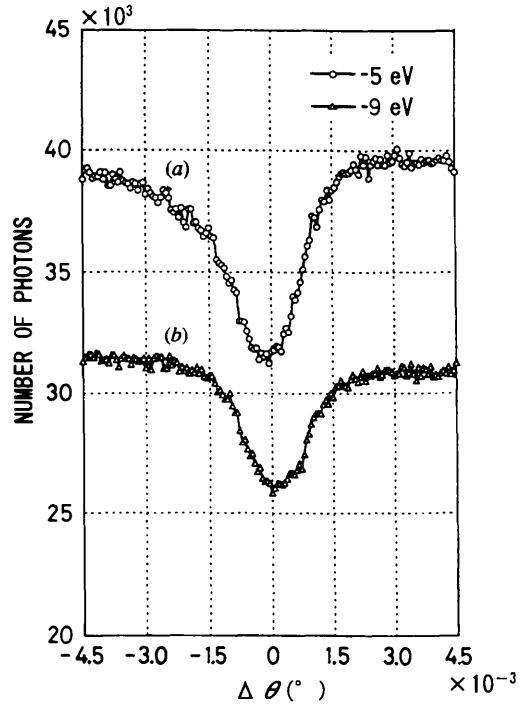

Fig. 8. The measured rocking curves of the transmitted beam for GaAs 200 for (*a*) -5 eV and (*b*) -9 eV from the Ga *K*-absorption edge.

For the X-ray energy between the Ga K-absorption edge and the As K-absorption edge, f''_{Ga} is much larger than f''_{As} and χ_{hi} is negative. Just above the Ga K-absorption edge, the relation $\delta = \pi$ means that χ_{hr} is positive and $\alpha_{hr} = 0$. Just across the absoption edge, the variation of χ_{hr} is almost symmetric because the dispersion curve of f' is almost symmetric with respect to the absorption-edge energy. If χ_{hr} is positive at the energy above the Ga K edge, it is also positive below the edge, which agrees with the result in §2.

4. Summary

We have measured the rocking curves of the transmitted beam for the GaAs 200 reflection in the symmetric Laue case and obtained the phase information of the X-ray polarizability or crystal structure factor as follows:

(i) For GaAs 200, the phase factor δ is either zero or π when either χ_{hr} or χ_{hi} is not zero. The rocking curve of the diffracted beam in the symmetric Laue case is symmetric with respect to $W = 0$ and does not depend on the change of δ. On the other hand, the rocking curve of the transmitted beam is asymmetric with respect to $W = 0$. The asymmetry reverses by changing δ from zero to π. This reversal effect has been measured in experiment by comparing the theoretical result. This means that we are able to determine whether the value of δ is zero or π by measuring the rocking curves.

(ii) We have determined the value of δ from the rocking curve for GaAs 200 in the energy range between Ga K- and As K-absorption edges. The value of δ is π just above the Ga K-absorption edge and is zero just below the As K-absorption edge. In this energy range, $f''_{Ga} \gg f''_{As}$, then χ_{hi} should be negative and α_{hi} is π. As δ is π just above the Ga K edge, χ_{hr} is positive ($\alpha_{hr} = 0$). Just below the As K edge, as δ is zero, χ_{hr} is negative ($\alpha_{hr} = \pi$). These results are in good agreement with the theoretical prediction.

(iii) We have determined the energy at which the sign of χ_{hi} for the GaAs 200 reflection reverses just below the Ga K-absorption edge. The energy is 7 ± 2 eV below the Ga K edge, which is much lower than expected in theory, *i.e.* 0 eV by CLS and 3.7 eV by PH. This suggests that the calculated anomalous scattering factor is not reliable enough to reproduce the rocking curves very close to the absorption edge in the present case.

Fukamachi *et al.* (1993) measured the integrated reflection intensities of Ge 844 and reported that the sign of χ_{hr} changed just below the Ge K-absorption edge. However, they did not observe the change of the phase factor directly. By using the present method, we should observe the change of the phase factor, which is the subject of future work.

The authors thank Professor M. Tokonami for his helpful advice, Mr K. Ehara for preparing the sample, and I. Matsumoto and S. Sato for their help in preparing the computing programs and the data analyses.

References

Cromer, D. T. (1965). *Acta Cryst.* **18**, 17–23.
Cromer, D. T. & Liberman, J. (1970). *J. Chem. Phys.* **53**, 1891–1898.
Fukamachi, T. & Kawamura, T. (1993). *Acta Cryst.* A**49**, 384–388.
Fukamachi, T., Negishi, R. & Kawamura, T. (1994). *Acta Cryst.* A**50**, 475–480.
Fukamachi, T., Negishi, R. & Kawamura, T. (1995). *Acta Cryst.* A**51**, 253–258.
Fukamachi, T., Negishi, R., Yoshizawa, M., Ehara, K., Kawamura, T., Nakajima, T. & Zhao, Z. (1993). *Acta Cryst.* A**49**, 573–575.
Kato, N. (1992). *Acta Cryst.* A**48**, 829–834.
Matsushita, T., Ishikawa, T. & Oyanagi, H. (1986). *Nucl. Instrum. Methods*, A**246**, 377–379.
Parratt, L. G. & Hempstead. C. F. (1954). *Phys. Rev.* **94**, 1593–1600.
Sasaki, S. (1989). KEK Report 88-14 M/D, pp. 1–136. Photon Factory, Tsukuba, Ibaraki, Japan.
Yoshizawa, M., Fukamachi, T., Ehara, K., Kawamura, T. & Hayakawa, K. (1988). *Acta Cryst.* A**44**, 433–436.